AEM
Journals.ASM.org

Carbon Flux Analysis by ^{13}C Nuclear Magnetic Resonance To Determine the Effect of CO_2 on Anaerobic Succinate Production by *Corynebacterium glutamicum*

Dušica Radoš,[a] David L. Turner,[a] Luís L. Fonseca,[a]* Ana Lúcia Carvalho,[a] Bastian Blombach,[b] Bernhard J. Eikmanns,[c] Ana Rute Neves,[a]* Helena Santos[a]

Instituto de Tecnologia Química e Biológica, Universidade Nova de Lisboa, Oeiras, Portugal[a]; Institute for Biochemical Engineering, University of Stuttgart, Stuttgart, Germany[b]; Institute of Microbiology and Biotechnology, University of Ulm, Ulm, Germany[c]

Wild-type *Corynebacterium glutamicum* produces a mixture of lactic, succinic, and acetic acids from glucose under oxygen deprivation. We investigated the effect of CO_2 on the production of organic acids in a two-stage process: cells were grown aerobically in glucose, and subsequently, organic acid production by nongrowing cells was studied under anaerobic conditions. The presence of CO_2 caused up to a 3-fold increase in the succinate yield (1 mol per mol of glucose) and about 2-fold increase in acetate, both at the expense of L-lactate production; moreover, dihydroxyacetone formation was abolished. The redistribution of carbon fluxes in response to CO_2 was estimated by using ^{13}C-labeled glucose and ^{13}C nuclear magnetic resonance (NMR) analysis of the labeling patterns in end products. The flux analysis showed that 97% of succinate was produced via the reductive part of the tricarboxylic acid cycle, with the low activity of the oxidative branch being sufficient to provide the reducing equivalents needed for the redox balance. The flux via the pentose phosphate pathway was low (~5%) regardless of the presence or absence of CO_2. Moreover, there was significant channeling of carbon to storage compounds (glycogen and trehalose) and concomitant catabolism of these reserves. The intracellular and extracellular pools of lactate and succinate were measured by *in vivo* NMR, and the stoichiometry (H^+:organic acid) of the respective exporters was calculated. This study shows that it is feasible to take advantage of natural cellular regulation mechanisms to obtain high yields of succinate with *C. glutamicum* without genetic manipulation.

Corynebacterium glutamicum is a facultatively anaerobic (1) Gram-positive bacterium that occupies a prominent position among industrial microorganisms, primarily due to its outstanding performance in the production of L-amino acids. In fact, over 2 million tons of L-glutamate and L-lysine are produced per year by *C. glutamicum* fermentation (2, 3). In addition, it is a GRAS (generally regarded as safe) organism that is robust (osmotolerant and phage resistant), extensively studied with respect to metabolism and regulation, and amenable to genetic manipulation, for which a comprehensive toolbox is available (4). Under aerobic conditions, *C. glutamicum* is able to grow relatively fast to high cell densities in minimal medium. In contrast, in the absence of oxygen and nitrate, cell growth is negligible, while the ability to metabolize sugars is retained (5, 6). Thus, cells of *C. glutamicum* can be grown aerobically and subsequently used for fermentation of desired products under anoxic conditions, as demonstrated for L-alanine, L-valine, or isobutanol (7–10).

It is well known that *C. glutamicum* converts glucose into organic acids, i.e., L-lactic, succinic, and acetic acids, under oxygen deprivation (5, 6, 11). Lactate and succinate are important bulk chemicals with increasing industrial demand; hence, it is not surprising that a considerable research effort has been made to optimize their production from renewable feedstocks, such as biomass (12). Wild-type *C. glutamicum* is able to produce L-lactate from glucose with a high yield (1.79 mol per mol glucose) (11); moreover, it has been successfully engineered for the production of D-lactate and derived polyesters (13, 14). In contrast, succinate is a minor product of glucose metabolism by wild-type *C. glutamicum* (5, 6, 11). Recent studies have shown that the presence of bicarbonate increases succinate production considerably (5, 11), and this finding prompted a variety of genetic and environmental manipulations aimed at further production enhancement (15, 16). In particular, a high yield of succinate (1.67 mol/mol glucose) was achieved by using formate as an electron and CO_2 donor, but there is still need for improvement with regard to productivity and cost-effectiveness (15).

Obviously, the maximization of organic acid production implies the reduction of by-products, namely, by metabolic-engineering strategies. As demonstrated for the construction of effective amino acid producers, the success of engineering approaches depends on detailed knowledge of cellular metabolism, which necessarily includes quantitative information on carbon flux distribution throughout the network of metabolic pathways (17, 18). Over the last 2 decades, our team has taken advantage of the analytical power of nuclear magnetic resonance (NMR) and its

Received 23 December 2013 **Accepted** 27 February 2014
Published ahead of print 7 March 2014
Editor: A. M. Spormann
Address correspondence to Helena Santos, santos@itqb.unl.pt.
* Present address: Luís L. Fonseca, Integrative BioSystems Institute and the Wallace H. Coulter Department of Biomedical Engineering, Georgia Institute of Technology and Emory University, Atlanta, Georgia, USA; Ana Rute Neves, CED-Discovery, Chr Hansen A/S, Hørsholm, Denmark.
Supplemental material for this article may be found at http://dx.doi.org/10.1128/AEM.04189-13.

doi:10.1128/AEM.04189-13

unique noninvasive characteristics to study different aspects of metabolism directly in living cell suspensions (19–21). We set out to apply this methodology and to characterize *C. glutamicum* metabolism in the anaerobic production phase, in the presence and absence of CO_2, to obtain pointers for the design of strains with maximal succinate production.

Here, we report the use of ^{13}C NMR combined with specifically ^{13}C-labeled glucose to assess the impact of CO_2 on the metabolic flux distribution in wild-type *C. glutamicum* in the anaerobic production phase. Moreover, the intracellular pools of organic acids were monitored *in vivo* during the production phase. Our analysis shows that the flux through the pentose phosphate pathway (PPP) is small and not significantly altered by the CO_2 supply. In addition, succinate production proceeds largely via the reductive branch of the tricarboxylic acid (TCA) cycle, but a significant flux via the oxidative branch provides the reducing equivalents needed for the redox balance.

MATERIALS AND METHODS

Growth conditions. *C. glutamicum* strain ATCC 13032 (22) was the only organism used in this work. Cells were grown aerobically in the CGXII minimal medium described by Eikmanns et al. (23), modified as follows: 5 g liter^{-1} $(NH_4)_2SO_4$, 21 g liter^{-1} MOPS (3-[*N*-morpholino] propanesulfonic acid), 0.2 mg liter^{-1} biotin. The medium was supplemented with 4% (wt/vol) glucose. Growth experiments were performed at 30°C with constant agitation at 140 rpm in 2-liter baffled shake flasks. The medium was inoculated by addition of a preculture to an initial optical density at 600 nm (OD_{600}) of approximately 0.5; the initial pH value was 7.0. Precultures were grown for 8 h under the same conditions as the main cultures, except that 250-ml baffled shake flasks were used. In all cases, the medium volume was 1/10 of the flasks' total capacity. Growth was monitored by measuring the OD_{600}. A factor of 0.24 ± 0.01, determined from a dry weight (DW) (mg ml^{-1})-versus-OD_{600} curve, was used to convert the OD_{600} into dry weight (mg biomass ml^{-1}).

Preparation of cell suspensions. Cells were grown as described above and harvested 16 h after inoculation, at the beginning of the stationary phase (OD_{600} = 40 to 45); centrifuged (9,924 × *g*; 10 min; 4°C); and washed twice with an appropriate buffer {MES [2-(*N*-morpholino)ethanesulfonic acid] or PIPES [piperazine-*N*,*N*′-bis(2-ethanesulfonic acid)]; 10 mM at pH 7}. The resulting cell suspension was centrifuged (11,325 × *g*; 10 min; 4°C), and the pellet was resuspended to an OD_{600} of 100 (dense cell suspension) or 7.5 (diluted cell suspension) in 50 mM buffer (PIPES at pH 7 or MES at pH 5.7); SAG 5693 antifoam (approximately 15 to 20 μl per 50 ml of cell suspension; Union Carbide Chemicals and Plastics) and D_2O (6% [vol/vol]) were added to the dense cell suspensions for the *in vivo* NMR measurements.

***In vivo* NMR experiments.** *In vivo* NMR experiments were performed using the on-line system described by Neves et al. (19), which consists of an 80-ml bioreactor coupled to the NMR tube with a circulating system that allows noninvasive studies of metabolism under controlled conditions of pH, gas atmosphere, and temperature. Dense cell suspensions (OD_{600} = 100) were placed in the bioreactor and kept at 30°C. The pH was controlled at 7.0 or 5.7 by the automatic addition of 5 M NaOH. To achieve anaerobic conditions, argon, carbon dioxide (CO_2), or a mixture of CO_2 and nitrogen (20% [vol/vol] CO_2), was bubbled through the cell suspension in the bioreactor and also provided to the headspace of the NMR tube. Glucose specifically labeled with ^{13}C on C-1 (20 mM) was added to the cell suspension at time point zero. The time courses of glucose consumption, product formation, and changes in the pools of intracellular organic acids were monitored *in vivo*. When the substrate was exhausted, an NMR sample extract was prepared as described previously (19, 20). In brief, an aliquot of the cell suspension (6 ml) was passed through a French press: the resulting cell extract was incubated at 82°C (10 min) in a stoppered tube and cooled on ice, and cell debris and denatured macromolecules were removed by centrifugation (45,696 × *g*; 10 min at 4°C). The supernatant (NMR sample extract) was used for quantification of end products and minor metabolites. Samples were stored at −20°C until further analysis.

Quantification of end products and intracellular organic acids. Lactate was quantified in the NMR sample extract by ^1H NMR in an AMX300 (Bruker BioSpin GmbH) spectrometer. Formic acid (sodium salt) was added to the samples and used as an internal concentration standard. The concentrations of other metabolites were determined in fully relaxed ^{13}C spectra of the NMR sample extracts as described by Neves et al. (19). Due to the fast pulsing conditions used for acquiring *in vivo* ^{13}C spectra, correction factors were determined to convert peak intensities into concentrations. The correction factors for the resonances due to C-3 of intracellular lactate (0.60 ± 0.04) and C-2/C-3 of intracellular succinate (0.60 ± 0.02) were determined from the acquisition of fully and partially relaxed spectra of an NMR extract. The correction factors for C-3 of extracellular lactate (0.55 ± 0.02) and C-2/C-3 of extracellular succinate (0.57 ± 0.02) were determined as described above, except that PIPES buffer (50 mM; pH 7.0) containing succinate (50 mM) and lactate (60 mM) was used. The quantitative kinetic data for intracellular metabolites were calculated as described previously (19–21). Intracellular concentrations were calculated using a value of 1.4 μl mg (dry weight)$^{-1}$ for the intracellular volume of *C. glutamicum* (24). Although individual experiments are illustrated in each figure, each experiment was repeated at least twice. The values reported are averages of two experiments, and the uncertainty varied from ±2% to ±15% for the metabolite concentration and from ±1% to ±10% for the maximal glucose consumption rate (GCR).

Analysis of metabolic fluxes in the anaerobic phase (nongrowing cells). Diluted cell suspensions (OD_{600} = 7.5) prepared as described above were used to estimate the fluxes through the metabolic pathways operating under oxygen deprivation. The cell suspensions were kept at 30°C under a controlled pH of 7.0, and anaerobic conditions were ensured by bubbling argon or CO_2 through the suspension. Glucose (50 mM) specifically labeled with ^{13}C on C-1 or C-2, simultaneously labeled on C-1 and C-2, or uniformly labeled was added to the cell suspension at time point zero. Samples (1 ml) were withdrawn at time point zero and periodically for 32 h and centrifuged (10,000 × *g*; 2 min at 4°C), and the supernatant solutions were saved at −20°C until further analysis. ^{13}C-labeled end products were quantified in the supernatants by ^{13}C NMR using tetramethylurea (99%) contained in a capillary as the concentration standard or by ^1H NMR using sodium formate as an internal standard. The total quantities of end products were determined from averages of 6 independent experiments and have a typical standard deviation of 3%.

^{13}C-glucose isotopomers were selected specifically to resolve the contributions of different pathways (25, 26). The labeling pattern of end products was analyzed, and a scheme including central metabolic pathways was constructed. This comprised glycolysis, the PPP, a reductive TCA cycle down to succinate and an oxidative TCA cycle also ending at succinate, lactate and acetate production from pyruvate (PYR), PYR/phosphoenolpyruvate (PEP) carboxylation, and oxaloacetate/malate conversion to pyruvate. The efflux of carbon at the level of glucose-6-phosphate toward carbon reserves (glycogen, trehalose, etc.) and the respective mobilization to glycolysis were also considered. PEP/PYR carboxylation reactions are lumped together, since the labeling patterns of PEP and pyruvate are indistinguishable; similarly, a single flux was considered for the decarboxylation reactions from oxaloacetate or malate. The two possible acetate-forming pathways from pyruvate are combined into a single pathway. All reactions in the reductive TCA cycle were considered reversible. The contribution of the glyoxylate shunt was neglected (see Discussion).

Deconvolution of overlapping intra- and extracellular organic acid resonances. Partial overlap of the intra- and extracellular organic acid resonances due to internal and external lactate hampered direct integration. Therefore, deconvolution of the relevant spectral region was per-

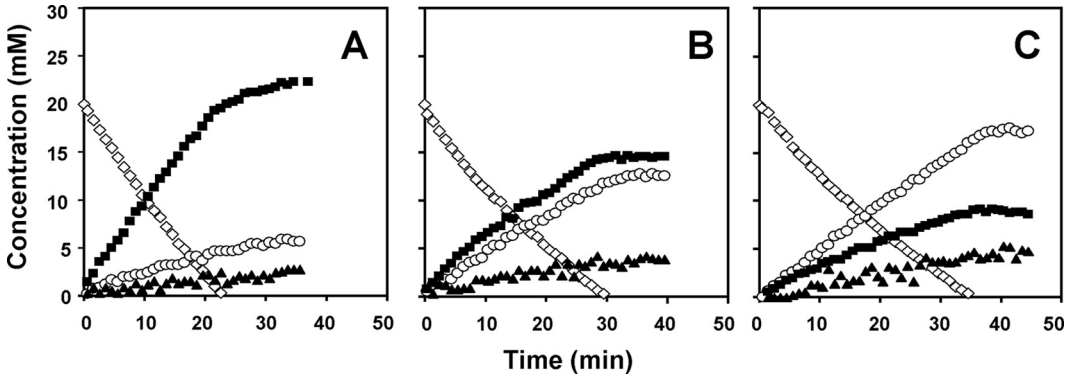

FIG 1 Time courses of glucose consumption and product accumulation during the metabolism of 20 mM [1-^{13}C]glucose in nongrowing cell suspensions of *C. glutamicum* (OD_{600} = 100). The experiments were monitored by *in vivo* ^{13}C NMR and carried out at 30°C, with pH controlled at 7.0 and bubbling no CO_2 (A), 20% CO_2 (B), or 100% CO_2 (C). Glucose consumption rates were 34.5 (A), 22.5 (B), and 21.2 (C) nmol min^{-1} mg $(DW)^{-1}$. Diamonds, glucose; circles, succinate; squares, lactate; triangles, acetate. Each panel represents a single experiment from a set of at least two similar replicates.

formed by fitting the sum of Lorentzian and Gaussian functions using Matlab V7.1 (Math Works, Natick, MA, USA).

Determination of *n*, the number of protons exported concomitantly with each molecule of organic acid. The total amounts of internal and external organic acids were fitted to exponential curves, which were used to calculate the *n* value, the number of protons exported concomitantly with each molecule of organic acid, numerically, as described by Carvalho et al. (21). The intracellular pH was determined by ^{31}P NMR, and the relative concentrations of the ionized forms were obtained using a pK_{a1} value of 4.2 and a pK_{a2} value of 5.6 for succinic acid.

NMR spectroscopy. All ^{13}C spectra were acquired at 125.77 MHz on a Bruker Avance II 500-MHz spectrometer (Bruker BioSpin GmbH) at 30°C. *In vivo* experiments were run using a quadruple-nucleus probe head, as described previously (19). ^{13}C NMR spectra of supernatants derived from diluted cell suspensions (OD_{600} = 7.5) were recorded using a ^{13}C-selective probe head, 32,000 data points, a 68° flip angle, and a repetition delay of 90.5 s. Tetramethylurea contained in a capillary was used as a concentration standard and also as a reference for chemical shifts (δ = 38.7 ppm).

Quantification of end products by HPLC. End products in supernatants derived from diluted cell suspensions or NMR sample extracts (dense cell suspensions) were also quantified by high-performance liquid chromatography (HPLC), using an apparatus equipped with a refractive index detector (Shodex RI-101; Showa Denko K. K., Japan) and an HPX-87H anion-exchange column (Bio-Rad Laboratories Inc., Hercules, CA, USA) at 60°C, with 5 mM H_2SO_4 as the elution fluid and a flow rate of 0.5 ml min^{-1}.

Chemicals. [1-^{13}C]glucose, [2-^{13}C]glucose, [1,2-^{13}C]glucose, and [U-^{13}C]glucose were obtained from Cambridge Isotope Laboratories, Inc. The SAG 5693 antifoam agent was from Union Carbide Chemicals and Plastics. Formic acid (sodium salt) and tetramethylurea were purchased from Merck Sharp & Dohme and Sigma-Aldrich, respectively. All other chemicals were reagent grade (Sigma-Aldrich and Merck Sharp & Dohme).

RESULTS

Effect of CO_2 on succinate production. *In vivo* ^{13}C NMR was used to characterize the metabolism of glucose in *C. glutamicum* ATCC 13032 at an OD_{600} of 100 and pH 7 under anaerobic conditions in (i) the absence of CO_2, (ii) 20% (vol/vol) CO_2, and (iii) pure CO_2 (Fig. 1). In the absence of CO_2, *C. glutamicum* produced lactate, succinate, and acetate from glucose, with lactate accounting for 1.22 mol per mol of glucose consumed (i.e., 61%) (Fig. 1A and Table 1). Replacement of argon by 20% (vol/vol) CO_2 (Fig. 1B) led to a decrease in lactate by about one-third (from 24.5 ± 3.1 mM to 14.6 ± 0.2 mM), while succinate production doubled (from 5.9 ± 0.2 to 11.8 ± 1.0 mM) (Fig. 1; see Table S1 in the supplemental

TABLE 1 Effect of CO_2 availability on anaerobic metabolism of glucose by *C. glutamicum* ATCC 13032[a]

OD_{600}	pH	% CO_2	Yield (mol mol Glc^{-1})[b]			GCR (nmol min^{-1} mg $[DW]^{-1}$)	^{13}C balance[c] (%)	Total C balance[d] (%)
			Lactate	Succinate	Acetate			
100	7.0	0	1.22 ± 0.16	0.29 ± 0.01	0.13 ± 0.02	34.5 ± 0.7	90.1 ± 6.5	141.1 ± 1.9
		20	0.73 ± 0.01	0.59 ± 0.05	0.19 ± 0.01	22.5 ± 2.1	83.8 ± 0.4	163.2 ± 20.6
		100	0.42 ± 0.01	0.87 ± 0.02	0.28 ± 0.01	21.2 ± 0.1	87.5 ± 1.2	173.2 ± 12.9
	5.7	0	1.19 ± 0.06	0.15 ± 0.01	0.06 ± 0.01	19.7 ± 0.4	86.5 ± 0.9	110.3 ± 11.3
		100	0.83 ± 0.04	0.41 ± 0.01	0.13 ± 0.01	18.4 ± 0.2	77.2 ± 3.4	110.6 ± 3.0
7.5	7.0	0	1.24 ± 0.06	0.03 ± 0.01	0.03 ± 0.01	25.0 ± 3.6	89.0 ± 2.8	103.2 ± 4.0
		100	0.56 ± 0.12	0.91 ± 0.11	0.26 ± 0.02	21.3 ± 1.4	79.7 ± 5.2	90.8 ± 5.8

[a] The initial concentrations of glucose were 20 and 50 mM for the experiments with dense and diluted cell suspensions, respectively. In dense cell suspensions (OD_{600} = 100), end products and glucose were determined online by *in vivo* NMR, while in diluted cell suspensions (OD_{600} = 7.5), they were measured by NMR and HPLC offline in the sample supernatants. The pH of the cell suspension was maintained at 7.0 or 5.7.

[b] Product yields were calculated assuming that [1-^{13}C]glucose was processed via the EMP pathway and that it produces a labeled and an unlabeled pyruvate molecule as follows: lactate yield = [3-^{13}C]lactate × 2/[1-^{13}C]glucose; acetate yield = [2-^{13}C]acetate × 2/[1-^{13}C]glucose; succinate yield = ([2,3-^{13}C]succinate × 2 + [1,4-^{13}C]succinate)/[1-^{13}C]glucose.

[c] The ^{13}C balance is the percentage of carbon in metabolized [^{13}C]glucose that is recovered in the fermentation products.

[d] The total carbon balances were calculated by summing the end product concentrations.

material). This trend was even more pronounced when the pure CO_2 was bubbled through the cell suspension (Fig. 1C and Table 1; see Table S1 in the supplemental material): lactate accounted for 21% of the glucose consumed (0.42 ± 0.01 mol per mol), corresponding to a ca. 3 times lower yield than in the absence of CO_2. Under pure CO_2, succinate was the major end product, reaching a maximal concentration of 17.5 ± 0.3 mM. CO_2 also had a positive effect on the acetate yield, which increased approximately 2-fold in the presence of 100% CO_2 compared to no added CO_2 (Table 1). Other minor products, including L-glutamate, L-alanine, α-ketoglutarate, trehalose, and glycogen, were detected under all conditions examined. A negative correlation was observed between the CO_2 supply and the GCR, which dropped from 34.5 ± 0.7 nmol min^{-1} mg $(DW)^{-1}$ to 22.5 ± 2.1 and 21.2 ± 0.1 nmol min^{-1} mg $(DW)^{-1}$ when 20% (vol/vol) CO_2 or 100% CO_2 was used, respectively (Table 1).

Carbon flux analysis in nongrowing cells based on ^{13}C NMR. The fundamental, as well as biotechnological, interest of finding that the succinate yield was strongly increased by CO_2 motivated us to characterize the redistribution of carbon fluxes induced by CO_2 in nongrowing cells (production stage). To this end, we relied on isotopomeric ^{13}C NMR analysis of end products from the anaerobic metabolism of glucose specifically labeled in suitable positions. The set of experiments was performed with diluted cell suspensions (OD_{600}, 7.5, compared to 100 used for *in vivo* NMR). The use of diluted cell suspensions was dictated by the need to reduce the contribution of unlabeled end products attributed to the concomitant metabolism of internal reserves, which would complicate the analysis of labeling patterns in end products. Indeed, in dense cell suspensions, the total amount of carbon recovered in end products was up to 70% greater than that expected from the supplied glucose (Table 1). Curiously, in the absence of CO_2, the succinate yield was around 10 times higher in the experiments with dense cell suspensions than in those with diluted cell suspensions. We speculate that this difference is related to a higher concentration of endogenous bicarbonate in thick suspensions, since CO_2 removal is less efficient.

Considering the fate of ^{13}C label derived from the several glucose isotopomers led to the conclusion that [2-^{13}C]glucose should provide optimal information on the activity of anaerobic pathways. Other isotopomers of glucose ([1-^{13}C]glucose, [1,2-^{13}C]glucose, and [U-^{13}C]glucose) gave additional information. By using [1-^{13}C]glucose and [U-^{13}C]glucose, we were able to track back-flux from the TCA cycle (oxaloacetate/malate) to 3-carbon units (PEP/PYR), and [1,2-^{13}C]glucose confirmed the PPP activity provided by the analysis of [2-^{13}C]glucose metabolism; all experiments were used to estimate the extent of metabolization of internal reserves. Because we were unable to analyze metabolites other than end products, namely, lactate, acetate, succinate, dihydroxyacetone (DHA), and glycerol, the model is necessarily highly simplified. Nonetheless, using the model, we were able to estimate and compare the activities of main pathways in response to CO_2, including the split PPP/glycolysis and the proportions of the reductive and oxidative branches in the TCA cycle.

NMR analysis of end products derived from metabolism of [2-^{13}C]glucose (Fig. 2; see Table S2 in the supplemental material) provided a straightforward and accurate way to determine division between the Embden-Meyerhof-Parnas (EMP) pathway and the PPP using the ^{13}C enrichments in C-2 and C-3 of lactate or DHA (25). Our data showed that the majority of glucose was metabolized via the EMP pathway in the absence of CO_2, while the activity of the PPP accounted for about 2% of the carbon taken up in glucose (Fig. 3A). The PPP flux was 5% in the presence of pure CO_2 (Fig. 3B). Without added CO_2, we observed a high level of production of DHA (21% of the total glucose carbon), while addition of CO_2 abolished DHA formation. Moreover, the presence of CO_2 had a strong impact on the distribution of fluxes at the pyruvate node, i.e., lactate production was reduced (from 65 to 25% of carbon input) while the remaining fluxes toward pyruvate dehydrogenase and PEP/PYR carboxylation reactions were clearly enhanced (about 6- and 16-fold, respectively).

Cells produced a small amount of [1,2-^{13}C]lactate (about 1% of total lactate) from the metabolism of [2-^{13}C]glucose, regardless of the CO_2 content of the atmosphere (Fig. 2D). The appearance of labeling on contiguous carbon atoms can originate from the reversible reactions catalyzed by transketolase and transaldolase in the PPP (25) or from the decarboxylation of 4-carbon dicarboxylic acids (oxaloacetate/malate), which are labeled in adjacent carbons (back-flux from oxaloacetate/malate to PEP/PYR). To clarify the origin of [1,2-^{13}C]lactate (derived from [2-^{13}C]glucose), we performed experiments with the supply of [1-^{13}C]glucose and [1,2-^{13}C]glucose; small amounts (about 0.5 mM) of [1-^{13}C]lactate and [1,2,3-^{13}C]lactate were detected, respectively (data not shown). This labeling pattern can be explained by a small percentage of fructose 6-phosphate produced through EMP that is directed to the reactions catalyzed by transketolase and transaldolase in the PPP. To confirm or rule out the occurrence of back-flux from oxaloacetate/malate to PEP/PYR, the alternative path that would produce the same labeling, we looked for [2-^{13}C]lactate in the end products derived from [1-^{13}C]glucose and also for [2,3-^{13}C]lactate derived from the metabolism of [U-^{13}C]glucose, following an approach eloquently described by McKinlay and Vieille in 2008 (27). The analysis showed only vestigial amounts of [2-^{13}C]lactate or [2,3-^{13}C]lactate (data not shown), meaning that the back-flux to pyruvate under a 100% CO_2 atmosphere is insignificant.

In the absence of added CO_2, the production of succinate was too low to estimate fluxes within the TCA cycle. However, the increase in succinate production induced by CO_2 enabled the characterization of the TCA cycle reactions in more detail. Approximately 97% (18.84 out of 19.58 mM) of the labeled succinate pool was enriched in either of the inner carbons (C-2 or C-3) (see Table S2 in the supplemental material), reflecting the prominent contribution of the reductive branch of the TCA cycle. The low proportion of succinate labeled on either C-1 or C-4 (3%) indicated a small but statistically significant contribution of the oxidative branch of the TCA cycle (see Discussion).

The proportions of succinate produced via the oxidative versus the reductive TCA cycle determined the amount of CO_2 released (1%; 3 mol per mol of succinate via oxidative TCA) and the amount incorporated through PEP/PYR carboxylation reactions (ca. 17%; 1 mol per mol of total succinate). Decarboxylation of pyruvate into acetate or acetyl-coenzyme A (CoA) and of 6-phosphogluconate (in the PPP) added to the loss of carbon through CO_2 (about 7% in total) (Fig. 3B). In experiments where pure CO_2 was provided, it is reasonable to assume that all of the incorporated CO_2 was unlabeled, whereas about one-third of the CO_2 lost in decarboxylation reactions was labeled on average across the various experiments. The gain (carboxylation reactions) and loss (decarboxylation reactions) of carbon were accounted for in both

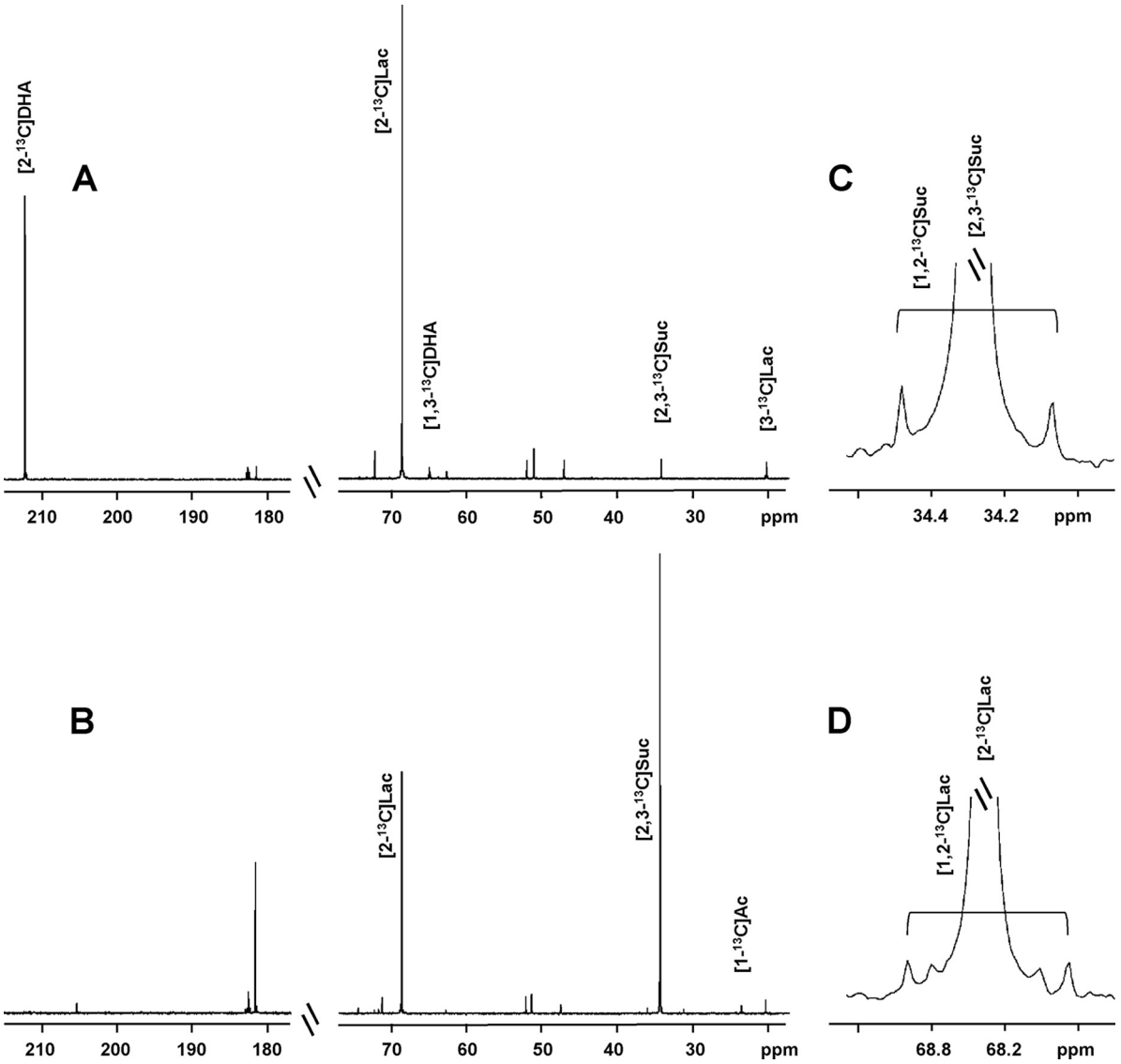

FIG 2 Relevant sections of ^{13}C NMR spectra of end products derived from the anaerobic metabolism of [2-^{13}C]glucose by diluted cell suspensions (OD_{600} = 7.5) of *C. glutamicum* in the absence of CO_2 (A) or the presence of 100% CO_2 (B, C, and D). Panels C and D are expansions of the resonance patterns due to [2,3-^{13}C]succinate and [2-^{13}C]lactate, respectively, in spectrum B. Lac, lactate; Suc, succinate; Ac, acetate. A representative experiment is depicted from a set of three replicates.

the ^{13}C and total carbon balances. The remaining loss of ^{13}C of about 10 to 20% was attributed to channeling of [^{13}C]glucose to reserve materials (glycogen, trehalose, etc.). The flux toward glycogen and trehalose was confirmed by *in vivo* NMR experiments that showed increasing resonances of glycogen and trehalose from the metabolism of C-1-labeled glucose (see Fig. S1 in the supplemental material). The difference between total C and ^{13}C balances, after accounting for incorporation of unlabeled CO_2, was attributed to catabolism of unlabeled intracellular reserves that had accumulated during growth (ca. 4% without CO_2 and 13% with 100% CO_2) (Fig. 3A and B). Therefore, there is carbon exchange with internal reserves and a net channeling of supplied glucose to the formation of storage compounds. The equations used to obtain the fluxes shown in Fig. 3 are listed in Fig. S2 in the supplemental material.

Intracellular pools of lactate and succinate, as determined by *in vivo* ^{13}C NMR. Production of organic acids by fermentation at low pH is highly desirable to facilitate downstream processing and to minimize waste products (28). Moreover, high intracellular pools of succinic and lactic acids may inhibit protein activity (21, 29). Therefore, we examined the effect of CO_2 on succinate production at a lower pH. Furthermore, at acidic pH, it is possible to monitor intracellular pools of organic acids noninvasively by ^{13}C NMR (21). The species of weak organic acids in solution are in fast exchange on the NMR time scale, thus giving rise to a single resonance whose chemical shift is determined by the proportion of the protonated and nonprotonated species, i.e., by pH. When the pH values of the intracellular and extracellular compartments are sufficiently different, the internal and external pools originate distinct resonances in the NMR spectrum. Here, the pH of the exter-

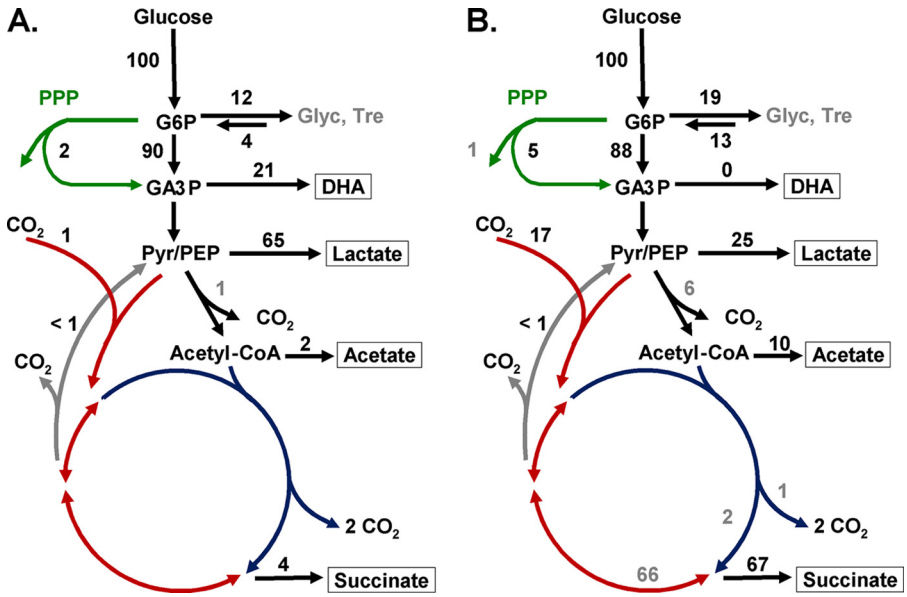

FIG 3 Scheme representing the reactions in the metabolic model used to estimate the flux distribution in nongrowing cells of *C. glutamicum* (OD_{600} = 7.5) with no supply of CO_2 (A) and with 100% CO_2 (B) at pH 7.0. To extract the minimal set of reactions operating under these conditions, we analyzed the ^{13}C labeling in end products from anaerobic metabolism of [1-^{13}C]glucose, [2-^{13}C]glucose, [1,2-^{13}C]glucose, and [U-^{13}C]glucose. Fluxes are shown as percentages in relation to the number of carbon atoms taken up as glucose. The lines with arrows represent fluxes in the central metabolism: PPP (green), EMP (black), reductive TCA (red), oxidative TCA (blue), and oxaloacetate/malate decarboxylation into PEP/PYR (gray). More precise values for fluxes are shown in Table S3 in the supplemental material.

nal solution was set at 5.7 based on the pH dependence of the chemical shift of succinate (C-2/C-3 resonance) and considering the neutrophilic character of *C. glutamicum*. A typical sequence of ^{13}C NMR spectra obtained during the metabolism of [1-^{13}C]glucose (Fig. 4) shows intense resonances due to extracellular succinate (δ, 33.4 ppm) and lactate (δ, 20.6 ppm). More importantly, two small resonances appear at 33.7 ppm and 20.7 ppm, which arise from these organic acids inside the cell (internal pH, approximately 6.3, as determined by ^{31}P NMR [data not shown]). The kinetics of glucose consumption and the buildup of intra- and extracellular pools under anaerobic conditions (with and without CO_2) are shown in Fig. 5. A shift in the external pH from 7.0 to 5.7 did not alter the nature of end products but led to a clear change in their proportions (Table 1). As for pH 7.0, CO_2 had a positive effect on succinate production (8.3 ± 0.2 mM compared to 3.1 ± 0.3 mM without CO_2), but lactate was the major end product at the lower pH regardless of the presence of pure CO_2 in the atmosphere. At pH 5.7, the GCR was impaired, and this negative effect was more pronounced in the absence of CO_2 (Table 1). Intracellular succinate and lactate pools increased steadily during glucose metabolism, reaching their maximal concentrations at the onset of glucose exhaustion. In the absence of CO_2, succinate and lactate reached intracellular levels of 17.2 ± 0.9 mM and 196.1 ± 28.4 mM, respectively (Fig. 5A). Under CO_2, the intracellular lactate pool decreased to 123.3 ± 18.4 mM, while the intracellular succinate concentration increased to 57.1 ± 1.7 mM. Except for small resonances assigned to fructose-1,6-bisphosphate, intermediate metabolite pools were below the detection limit of these experiments (around 3 mM).

DISCUSSION

In this study, we investigated the effect of CO_2 on anaerobic organic acid formation by wild-type *C. glutamicum* and found that the succinate yield increased 3-fold to 1 mol succinate per mol glucose in the presence of CO_2. This experimental yield is significantly higher than those reported in the literature for wild-type *C. glutamicum*, which do not exceed 0.44 mol succinate per mol glucose (11, 30). Moreover, it is significant even compared with engineered *C. glutamicum* strains that show succinate yields between 1.02 and 1.67 mol/mol glucose (15, 16, 31, 32).

The increase in the succinate yield prompted us to characterize the underlying redistribution of carbon fluxes. Analysis of enrichment on C-2 and C-3 of lactate derived from [2-^{13}C]glucose showed a low proportion of flux through the PPP in relation to glycolysis, and this split ratio was only slightly increased in the presence of CO_2. To our knowledge, this is the first estimation of the contribution of the PPP in *C. glutamicum* under oxygen depletion conditions. The low contribution of the PPP flux corroborates the view that in *C. glutamicum* the activity of this pathway is controlled by the demand for NADPH (33), which is naturally low in nongrowing cells, producing mainly organic acids. Accordingly, during the valine production phase of a recombinant L-valine-producing strain of *C. glutamicum* (nongrowing cells with oxygen supplied), the carbon flux was fully directed to the PPP to match the high demand for NADPH associated with the synthesis of this amino acid (2 mol NADPH per valine produced) (18).

In the absence of added CO_2, besides lactate, cells produced considerable amounts of DHA, which indicates the presence of a metabolic bottleneck at the level of glyceraldehyde-3-phosphate dehydrogenase, most likely due to enzyme inhibition by a high $NADH/NAD^+$ ratio (34). Significantly, this redox imbalance was abolished under succinate-producing conditions, since the reductive part of the TCA cycle provides a sink for reducing equivalents, and hence, DHA was not produced.

Succinate production occurred mainly via PEP/PYR carboxy-

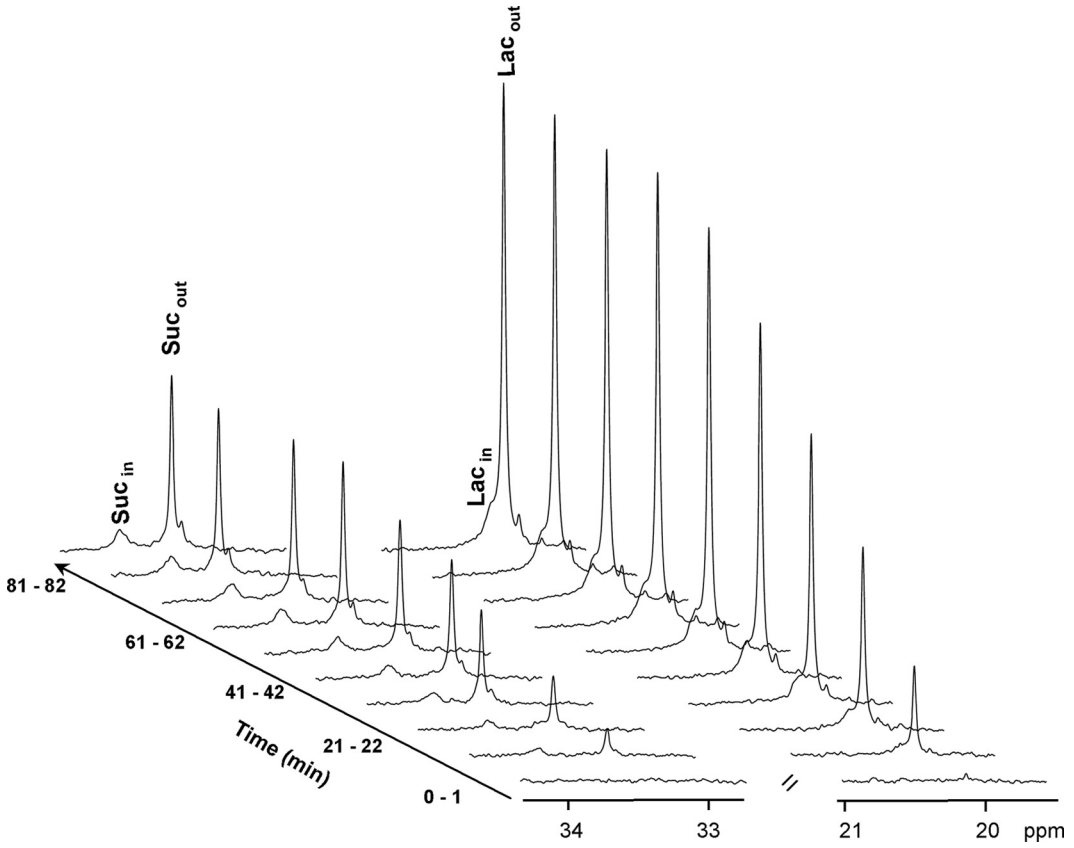

FIG 4 Sequences of ^{13}C NMR spectra acquired during glucose metabolism by dense cell suspensions (OD_{600} = 100) of *C. glutamicum* at pH 5.7 under a 100% CO_2 atmosphere. The resonances due to intra- and extracellular succinate and lactate are depicted. Suc_{in}, intracellular succinate; Suc_{out}, extracellular succinate; Lac_{in}, intracellular lactate; Lac_{out}, extracellular lactate. A single experiment is depicted from two independent replicates with high reproducibility.

lation and the reductive TCA cycle. However, the detection of ^{13}C labeling on the outer carbons of succinate (Fig. 2; see Table S2 in the supplemental material) denotes the operation of the oxidative path and/or the glyoxylate shunt. These two pathways lead to identical labeling patterns on succinate, so their individual contributions cannot be resolved. We assumed that the flux through the glyoxylate shunt is negligible under the experimental conditions used in this study, based on the following information: the activity of isocitrate lyase is absent in *C. glutamicum* during anaerobic glucose metabolism (11), and succinate is an effective inhibitor of isocitrate lyase (inhibition constant, 1.48 mM) (29). Therefore, it seems reasonable to neglect the glyoxylate shunt contribution in our metabolic model, which was designed for cells producing high levels of succinate, under anaerobic nongrowing conditions.

Activity of the full oxidative branch of the TCA cycle makes sense in view of the overall redox balance. For calculation of the redox balance, all three reduced cofactors (NADH, NADPH, and MQH_2) were considered equivalent electron-reducing units (35, 36). It is rewarding to find that the small flux through the oxidative TCA cycle (2 C atoms succinate for each 100 C atoms glucose taken up), estimated from the ^{13}C enrichment on C-1/C-4 of succinate, provides the balance of the reducing power needed for succinate production. Indeed, the calculation of the overall redox balance would be exactly 100% with a flux of 3.5 (instead of 2) carbons through the oxidative TCA cycle, which is a difference within the uncertainty of the data. However, a large deficit in reducing capacity (up to 20%) would occur if the glyoxylate shunt was active and the oxidative branch inoperative. Low contributions of the oxidative branch to anaerobic succinate production have also been reported in *Escherichia coli* and in *Basfia succinoproducens* and appear to be required for optimal production in nongrowing cells (37, 38). The operation of the oxidative branch of the TCA cycle implies a cost in terms of CO_2 loss; thus, Zhu et al. (32) constructed a *C. glutamicum* strain with overexpression of the genes involved in the glyoxylate shunt, but this strategy alone was not satisfactory, as the yield was essentially unchanged (1.21 to 1.23 mol/mol glucose).

The experiments with [1-^{13}C]glucose and [U-^{13}C]glucose showed that back-flux from oxaloacetate/malate to PEP/PYR is insignificant under a 100% CO_2 atmosphere. This was unexpected, given that the PEP/PYR/oxaloacetate node shows great flexibility in *C. glutamicum* cells, at least in the presence of oxygen (18, 39). There are three possible routes through which oxaloacetate/malate can be decarboxylated into PEP/PYR: (i) oxaloacetate decarboxylase, which is inhibited by succinate (40); (ii) PEP carboxykinase, which is downregulated under oxygen deprivation (41); and (iii) the malic enzyme, which is overexpressed under oxygen deprivation (41). Therefore, it appears that the malic enzyme has very low activity in the decarboxylating direction, probably because of a low requirement for NADPH. Actually, having the malic enzyme acting in the malate-forming direction, as previously suggested (42), would provide a sink for NADPH pro-

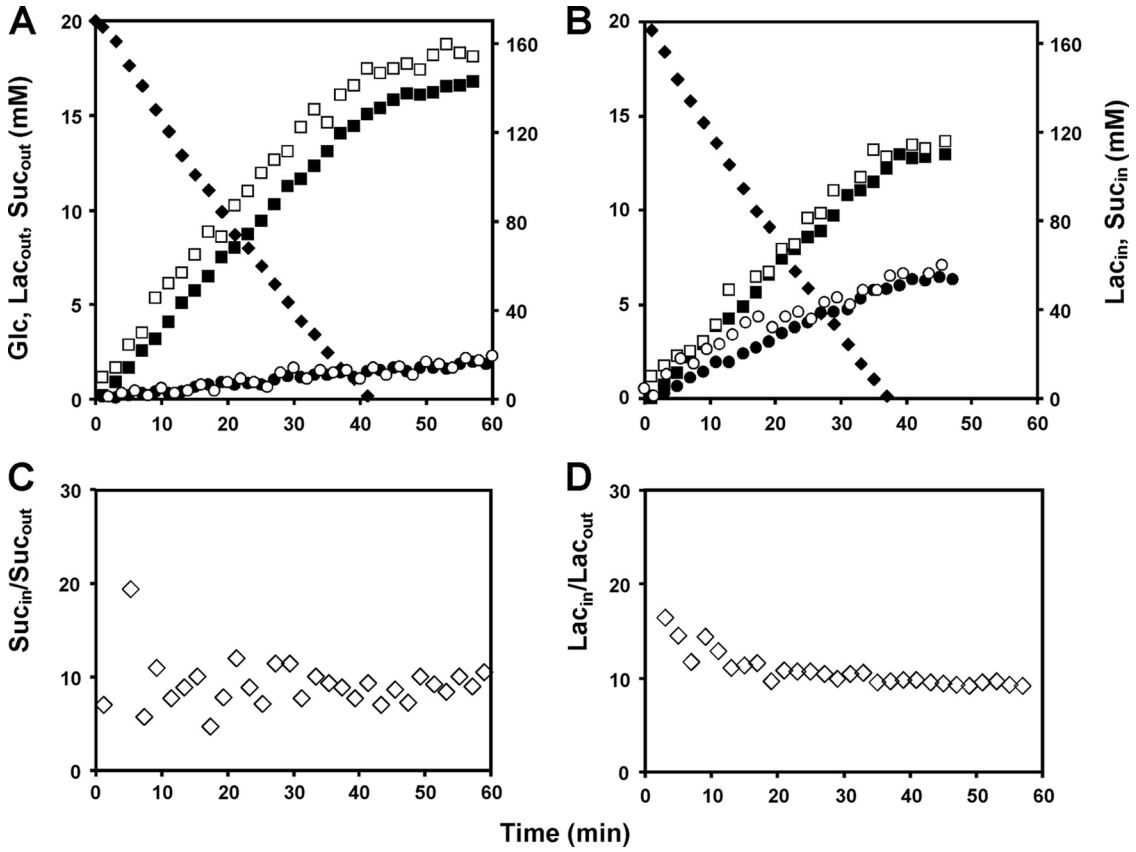

FIG 5 (A and B) Time courses for consumption of glucose (20 mM) and buildup of intra- and extracellular pools of lactate and succinate determined from the sequences of spectra shown in Fig. 4 in the absence of CO_2 (A) and in the presence of 100% CO_2 (B). Diamonds, glucose; solid squares, extracellular lactate; open squares, intracellular lactate; solid circles, extracellular succinate; open circles, intracellular succinate. (C and D) Plots of the intracellular succinate/extracellular succinate ratio (C) and the intracellular lactate/extracellular lactate ratio (D). Each panel represents a single experiment from a set of at least two similar replicates.

duced in the PPP, a useful feature, since the bacterium lacks NADPH-NAD^+ transhydrogenase activity (43, 44).

The difference between the recovery of ^{13}C and that of total carbon (Table 1) deserves further discussion. In addition to the obvious dilution of label resulting from ^{12}C incorporation from CO_2 in PEP/PYR carboxylation reactions, one should consider the contribution of unlabeled internal reserves. *C. glutamicum* can store glycogen and maltodextrins during growth (45), as well as trehalose (46), and the catabolism of these components concomitantly with the metabolism of added labeled glucose leads to ^{13}C dilution, as demonstrated by the presence of unlabeled end products when uniformly labeled glucose was provided. This phenomenon has been observed in bacteria and yeast, which showed fast mobilization of carbohydrate storage pools (47, 48). Moreover, the reverse flux from labeled glucose to reserves was apparent from the buildup of labeled glycogen and trehalose (see Fig. S1 in the supplemental material). Therefore, our model takes into account that both the utilization of internal reserves and storage of labeled glucose occur in the presence and absence of CO_2. According to this model, 12% and 19% of labeled glucose was stored, and unlabeled reserves (4% and 13% of C atoms taken up as glucose) were channeled to catabolism.

Lowering the pH from neutral to 5.7 had a strong negative effect on the GCR. Furthermore, the decrease in metabolic efficiency was accompanied by a decline in the succinate yield. As the cells were grown under identical conditions, transcriptional or proteomic effects are unlikely to occur, and the metabolic effects are ascribed to an immediate impact of pH on the efficiency of glucose transporters and/or cytoplasmic enzymes. The lack of effect at the transcriptional level has been demonstrated in *Lactococcus lactis* under similar experimental conditions (21). Despite the poor performance of *C. glutamicum* at acidic pH, we decided to measure the intracellular pools of organic acids, seeking information on eventual constraints at the level of organic acid export systems. The average number, *n*, of protons exported with the lactate or succinate anions was determined directly from the kinetics of accumulation of intra- and extracellular organic acids (21). During glucose consumption in a CO_2 atmosphere, *n* was maintained close to 1.4 in the case of lactate and varied only slightly (between 2.7 and 2.3) in the case of succinate, indicating lack of inhibition of exporters by the acid intracellular pools, which are actually much lower than those observed in *L. lactis* (up to 0.7 M lactate). Both for lactate and succinate, the intracellular/extracellular pool ratio rose rapidly to about 10 during glucose utilization (Fig. 5). Succinate exporters have been identified in several *C. glutamicum* strains, but their detailed characterization is lacking (49, 50). We speculate that, although cultivated at neutral pH, the organism is well adjusted to sustain the observed production fluxes at pH 5.7; moreover, the ability to maintain a high

concentration gradient across the cell membrane creates a favorable contribution to the energetics of the efflux processes.

In conclusion, this study demonstrates that the supply of CO_2 to wild-type *C. glutamicum* caused an important redistribution of the central metabolic fluxes, resulting in up to 3-fold improvement in the succinate yield without involvement of genetic manipulation. Succinate was produced largely via the reductive part of the TCA cycle, but there was also a significant flux through the oxidative part to meet the redox balance. Under production conditions (no growth and lack of oxygen), the split ratio between the PPP and glycolysis was low (around 5%) and independent of CO_2 availability, indicating that the flux via the PPP is primarily controlled by NADPH demand. The metabolism of glucose-grown cells of *C. glutamicum* seemed well tuned to produce succinate at a high yield with straightforward manipulation of environmental conditions and taking advantage of cellular regulation mechanisms. However, further effort should be directed to improving the rate of glucose consumption.

ACKNOWLEDGMENTS

We acknowledge Ana Mingote for technical assistance.

This work was supported by Fundação para a Ciência e a Tecnologia, Portugal (FCT), and FEDER, project ERA-IB/BIO/0002/2008, and by the BMELV (FNR grant 220-095-08A; BioProChemBB project). D.R. and L.L.F. acknowledge FCT for the award of Ph.D. (SFRH/BD/73265/2010) and postdoctoral (SFRH/BPD/26902/2006) grants, respectively. The NMR spectrometers are part of the National NMR Facility, supported by Fundação para a Ciência e a Tecnologia (RECI/BBB-BQB/0230/2012).

REFERENCES

1. **Nishimura T, Vertès AA, Shinoda Y, Inui M, Yukawa H.** 2007. Anaerobic growth of *Corynebacterium glutamicum* using nitrate as a terminal electron acceptor. Appl. Microbiol. Biotechnol. **75:**889–897. http://dx.doi.org/10.1007/s00253-007-0879-y.
2. **Shimizu H, Hirasava T.** 2007. Production of glutamate and glutamate-related amino acids: molecular mechanism analysis and metabolic engineering, p 2–29. *In* Wendisch VF (ed), Amino acid biosynthesis: pathways, regulation and metabolic engineering. Microbiology Monographs, vol 5. Springer, New York, NY.
3. **Becker J, Wittmann C.** 2012. Bio-based production of chemicals, materials and fuels: *Corynebacterium glutamicum* as versatile cell factory. Curr. Opin. Biotechnol. **23:**631–640. http://dx.doi.org/10.1016/j.copbio.2011.11.012.
4. **Eggeling L, Reyes O.** 2005. Experiments, p 535–566. *In* Eggeling L, Bott M (ed), Handbook of *Corynebacterium glutamicum*. Taylor & Francis, Boca Raton, FL.
5. **Okino S, Inui M, Yukawa H.** 2005. Production of organic acids by *Corynebacterium glutamicum* under oxygen deprivation. Appl. Microbiol. Biotechnol. **68:**475–480. http://dx.doi.org/10.1007/s00253-005-1900-y.
6. **Dominguez H, Nezondet C, Lindley ND, Cocaign M, National I, De Rangueil CS.** 1993. Modified carbon flux during oxygen limited growth of *Corynebacterium glutumicum* and the consequences for amino acid overproduction. Biotechnol. Lett. **15:**449–454. http://link.springer.com/article/10.1007%2FBF00129316#page-1.
7. **Yamamoto S, Gunji W, Suzuki H, Toda H, Suda M, Jojima T, Inui M, Yukawa H.** 2012. Overexpression of genes encoding glycolytic enzymes in *Corynebacterium glutamicum* enhances glucose metabolism and alanine production under oxygen deprivation conditions. Appl. Environ. Microbiol. **78:**4447–4457. http://dx.doi.org/10.1128/AEM.07998-11.
8. **Hasegawa S, Suda M, Uematsu K, Natsuma Y, Hiraga K, Jojima T, Inui M, Yukawa H.** 2013. Engineering of *Corynebacterium glutamicum* for high-yield L-valine production under oxygen deprivation conditions. Appl. Environ. Microbiol. **79:**1250–1257. http://dx.doi.org/10.1128/AEM.02806-12.
9. **Yamamoto S, Suda M, Niimi S, Inui M, Yukawa H.** 2013. Strain optimization for efficient isobutanol production using *Corynebacterium glutamicum* under oxygen deprivation. Biotechnol. Bioeng. **110:**2938–2948. http://dx.doi.org/10.1002/bit.24961.
10. **Blombach B, Riester T, Wieschalka S, Ziert C, Youn J-W, Wendisch VF, Eikmanns BJ.** 2011. *Corynebacterium glutamicum* tailored for efficient isobutanol production. Appl. Environ. Microbiol. **77:**3300–3310. http://dx.doi.org/10.1128/AEM.02972-10.
11. **Inui M, Murakami S, Okino S, Kawaguchi H, Vertès AA, Yukawa H.** 2004. Metabolic analysis of *Corynebacterium glutamicum* during lactate and succinate productions under oxygen deprivation conditions. J. Mol. Microbiol. Biotechnol. **7:**182–196. http://dx.doi.org/10.1159/000079827.
12. **Bozell JJ, Petersen GR.** 2010. Technology development for the production of biobased products from biorefinery carbohydrates—the US Department of Energy's "Top 10" revisited. Green Chem. **12:**539–554. http://dx.doi.org/10.1039/b922014c.
13. **Okino S, Suda M, Fujikura K, Inui M, Yukawa H.** 2008. Production of D-lactic acid by *Corynebacterium glutamicum* under oxygen deprivation. Appl. Microbiol. Biotechnol. **78:**449–454. http://dx.doi.org/10.1007/s00253-007-1336-7.
14. **Song Y, Matsumoto K, Yamada M, Gohda A, Brigham CJ, Sinskey AJ, Taguchi S.** 2012. Engineered *Corynebacterium glutamicum* as an endotoxin-free platform strain for lactate-based polyester production. Appl. Microbiol. Biotechnol. **93:**1917–1925. http://dx.doi.org/10.1007/s00253-011-3718-0.
15. **Litsanov B, Brocker M, Bott M.** 2012. Toward homosuccinate fermentation: metabolic engineering of *Corynebacterium glutamicum* for anaerobic production of succinate from glucose and formate. Appl. Environ. Microbiol. **78:**3325–3337. http://dx.doi.org/10.1128/AEM.07790-11.
16. **Okino S, Noburyu R, Suda M, Jojima T, Inui M, Yukawa H.** 2008. An efficient succinic acid production process in a metabolically engineered *Corynebacterium glutamicum* strain. Appl. Microbiol. Biotechnol. **81:**459–464. http://dx.doi.org/10.1007/s00253-008-1668-y.
17. **Kiefer P, Heinzle E, Zelder O, Wittmann C.** 2004. Comparative metabolic flux analysis of lysine-producing *Corynebacterium glutamicum* cultured on glucose or fructose. Appl. Environ. Microbiol. **70:**229–239. http://dx.doi.org/10.1128/AEM.70.1.229-239.2004.
18. **Bartek T, Blombach B, Lang S, Eikmanns BJ, Wiechert W, Oldiges M, Nöh K, Noack S.** 2011. Comparative ^{13}C-metabolic flux analysis of PDHC-deficient L-valine producing *Corynebacterium glutamicum*. Appl. Environ. Microbiol. **77:**6644–6652. http://dx.doi.org/10.1128/AEM.00575-11.
19. **Neves AR, Ramos A, Nunes MC, Kleerebezem M, Hugenholtz J, De Vos WM, Almeida J, Santos H.** 1999. *In vivo* nuclear magnetic resonance studies of glycolytic kinetics in *Lactococcus lactis*. Biotechnol. Bioeng. **64:**200–212. http://dx.doi.org/10.1002/(SICI)1097-0290(19990720)64:2<200::AID-BIT9>3.0.CO;2-K.
20. **Neves AR, Ventura R, Mansour N, Shearman C, Gasson MJ, Maycock C, Ramos A, Santos H.** 2002. Is the glycolytic flux in *Lactococcus lactis* primarily controlled by the redox charge? Kinetics of NAD(+) and NADH pools determined *in vivo* by ^{13}C NMR. J. Biol. Chem. **277:**28088–28098. http://dx.doi.org/10.1074/jbc.M202573200.
21. **Carvalho AL, Turner DL, Fonseca LL, Solopova A, Catarino T, Kuipers OP, Voit EO, Neves AR, Santos H.** 2013. Metabolic and transcriptional analysis of acid stress in *Lactococcus lactis*, with a focus on the kinetics of lactic acid pools. PLoS One **8:**e68470. http://dx.doi.org/10.1371/journal.pone.0068470.
22. **Kinoshita S, Nakayama K, Akita S.** 1958. Taxonomical study of glutamic acid accumulating bacteria, Micrococcus glutamicus nov. sp. Bull. Soc. Chem. Soc. Japan **22:**176–185.
23. **Eikmanns BJ, Metzger M, Reinscheid D, Kircher M, Sahm H.** 1991. Amplification of three threonine biosynthesis genes in *Corynebacterium glutamicum* and its influence on carbon flux in different strains. Appl. Microbiol. Biotechnol. **34:**617–622. http://dx.doi.org/10.1007/BF00167910.
24. **Krämer R, Lambert C, Hoischen C, Ebbighausen H.** 1990. Uptake of glutamate in *Corynebacterium glutamicum*. Kinetic properties and regulation by internal pH and potassium. Eur. J. Biochem. **194:**929–935.
25. **Schrader MC, Eskey CJ, Simplaceanu V, Ho C.** 1993. A carbon-13 nuclear magnetic resonance investigation of the metabolic fluxes associated with glucose metabolism in human erythrocytes. Biochim. Biophys. Acta **1182:**162–178. http://dx.doi.org/10.1016/0925-4439(93)90138-Q.
26. **Klapa M, Park S, Sinskey A, Stephanopoulos G.** 1999. Metabolite and isotopomer balancing in the analysis of metabolic cycles. I. Theory. Biotechnol. Bioeng. **62:**375–391.
27. **McKinlay JB, Vieille C.** 2008. ^{13}C-metabolic flux analysis of *Actinobacillus succinogenes* fermentative metabolism at different $NaHCO_3$ and

H_2 concentrations. Metab. Eng. **10:**55–68. http://dx.doi.org/10.1016/j.ymben.2007.08.004.
28. **Straathof AJJ.** 2013. Transformation of biomass into commodity chemicals using enzymes or cells. Chem. Rev. http://dx.doi.org/10.1021/cr400309c.
29. **Reinscheid DJ, Eikmanns BJ, Sahm H.** 1994. Characterization of the isocitrate lyase gene from *Corynebacterium glutamicum* and biochemical analysis of the enzyme. J. Bacteriol. **176:**3474–3483.
30. **Yamamoto S, Sakai M, Inui M, Yukawa H.** 2011. Diversity of metabolic shift in response to oxygen deprivation in *Corynebacterium glutamicum* and its close relatives. Appl. Microbiol. Biotechnol. **90:**1051–1061. http://dx.doi.org/10.1007/s00253-011-3144-3.
31. **Wieschalka S, Blombach B, Bott M, Eikmanns BJ.** 2013. Bio-based production of organic acids with *Corynebacterium glutamicum*. Microb. Biotechnol. **6:**87–102. http://dx.doi.org/10.1111/1751-7915.12013.
32. **Zhu N, Xia H, Yang J, Zhao X, Chen T.** 2013. Improved succinate production in *Corynebacterium glutamicum* by engineering glyoxylate pathway and succinate export system. Biotechnol. Lett. http://dx.doi.org/10.1007/s10529-013-1376-2.
33. **Marx A, Eikmanns BJ, Sahm H, De Graaf AA, Eggeling L.** 1999. Response of the central metabolism in *Corynebacterium glutamicum* to the use of an NADH-dependent glutamate dehydrogenase. Metab. Eng. **1:**35–48. http://dx.doi.org/10.1006/mben.1998.0106.
34. **Even S, Garrigues C, Loubiere P, Lindley ND, Cocaign-Bousquet M.** 1999. Pyruvate metabolism in *Lactococcus lactis* is dependent upon glyceraldehyde-3-phosphate dehydrogenase activity. Metab. Eng. **1:**198–205. http://dx.doi.org/10.1006/mben.1999.0120.
35. **Bott M.** 2003. The respiratory chain of *Corynebacterium glutamicum*. J. Biotechnol. **104:**129–153. http://dx.doi.org/10.1016/S0168-1656(03)00144-5.
36. **Genda T, Nakamatsu T, Ozak H.** 2003. Purification and characterization of malate dehydrogenase from *Corynebacterium glutamicum*. J. Biosci. Bioeng. **95:**562–566. http://dx.doi.org/10.1016/S1389-1723(03)80162-7.
37. **Sánchez AM, Bennett GN, San K-Y.** 2006. Batch culture characterization and metabolic flux analysis of succinate-producing Escherichia coli strains. Metab. Eng. **8:**209–226. http://dx.doi.org/10.1016/j.ymben.2005.11.004.
38. **Becker J, Reinefeld J, Stellmacher R, Schäfer R, Lange A, Meyer H, Lalk M, Zelder O, von Abendroth G, Schröder H, Haefner S, Wittmann C.** 2013. Systems-wide analysis and engineering of metabolic pathway fluxes in bio-succinate producing *Basfia succiniciproducens*. Biotechnol. Bioeng. **110:**3013–3023. http://dx.doi.org/10.1002/bit.24963.
39. **Wendisch VF, De Graaf AA, Sahm H, Eikmanns BJ.** 2000. Quantitative determination of metabolic fluxes during coutilization of two carbon sources: comparative analyses with *Corynebacterium glutamicu*m during growth on acetate and/or glucose. J. Bacteriol. **182:**3088–3096. http://dx.doi.org/10.1128/JB.182.11.3088-3096.2000.
40. **Jetten MS, Sinskey AJ.** 1995. Purification and properties of oxaloacetate decarboxylase from *Corynebacterium glutamicum*. Antonie Van Leeuwenhoek **67:**221–227. http://dx.doi.org/10.1007/BF00871217.
41. **Inui M, Suda M, Okino S, Nonaka H, Puskás LG, Vertès AA, Yukawa H.** 2007. Transcriptional profiling of *Corynebacterium glutamicum* metabolism during organic acid production under oxygen deprivation conditions. Microbiology **153:**2491–2504. http://dx.doi.org/10.1099/mic.0.2006/005587-0.
42. **Gourdon P, Baucher MF, Lindley ND, Guyonvarch A.** 2000. Cloning of the malic enzyme gene from *Corynebacterium glutamicum* and role of the enzyme in lactate metabolism. Appl. Environ. Microbiol. **66:**2981–2987. http://dx.doi.org/10.1128/AEM.66.7.2981-2987.2000.
43. **Blombach B, Buchholz J, Busche T, Kalinowski J, Takors R.** 2013. Impact of different CO_2/$HCO_3^{(-)}$ levels on metabolism and regulation in *Corynebacterium glutamicum*. J. Biotechnol. **168:**331–340. http://dx.doi.org/10.1016/j.jbiotec.2013.10.005.
44. **Kabus A, Georgi T, Wendisch VF, Bott M.** 2007. Expression of the *Escherichia coli pntAB* genes encoding a membrane-bound transhydrogenase in *Corynebacterium glutamicum* improves L-lysine formation. Appl. Microbiol. Biotechnol. **75:**47–53. http://dx.doi.org/10.1007/s00253-006-0804-9.
45. **Seibold G, Dempf S, Schreiner J, Eikmanns BJ.** 2007. Glycogen formation in *Corynebacterium glutamicum* and role of ADP-glucose pyrophosphorylase. Microbiology **153:**1275–1285. http://dx.doi.org/10.1099/mic.0.2006/003368-0.
46. **Wolf A, Krämer R, Morbach S.** 2003. Three pathways for trehalose metabolism in *Corynebacterium glutamicum* ATCC13032 and their significance in response to osmotic stress. Mol. Microbiol. **49:**1119–1134. http://dx.doi.org/10.1046/j.1365-2958.2003.03625.x.
47. **Matheron C, Delort A, Gaudet G.** 1998. ^{13}C and ^{1}H nuclear magnetic resonance study of glycogen futile cycling in strains of the genus *Fibrobacter*. Appl. Environ. Microbiol. **64:**74–81.
48. **Aboka FO, Heijnen JJ, Van Winden WA.** 2009. Dynamic ^{13}C-tracer study of storage carbohydrate pools in aerobic glucose-limited *Saccharomyces cerevisiae* confirms a rapid steady-state turnover and fast mobilization during a modest stepup in the glucose uptake rate. FEMS Yeast Res. **9:**191–201. http://dx.doi.org/10.1111/j.1567-1364.2008.00465.x.
49. **Huhn S, Jolkver E, Krämer R, Marin K.** 2011. Identification of the membrane protein SucE and its role in succinate transport in *Corynebacterium glutamicum*. Appl. Microbiol. Biotechnol. **89:**327–335. http://dx.doi.org/10.1007/s00253-010-2855-1.
50. **Fukui K, Koseki C, Yamamoto Y, Nakamura J, Sasahara A, Yuji R, Hashiguchi K, Usuda Y, Matsui K, Kojima H, Abe K.** 2011. Identification of succinate exporter in *Corynebacterium glutamicum* and its physiological roles under anaerobic conditions. J. Biotechnol. **154:**25–34. http://dx.doi.org/10.1016/j.jbiotec.2011.03.010.